International Journal of GEOMATE, Nov., 2023 Vol.25, Issue 111, pp. 104-112
ISSN: 2186-2982 (P), 2186-2990 (O), Japan, DOI: https://doi.org/10.21660/2023.111.4019
Geotechnique, Construction Materials and Environment

LIQUEFACTION POTENTIAL IN WATERFRONT AREA OF LABUAN BAJO BASED ON EARTHQUAKE RETURN PERIOD

Vicky Pratama[1], *Hary Christady Hardiyatmo[1] and Ashar Saputra[1]

[1]Department of Civil and Environmental Engineering, Universitas Gadjah Mada, Indonesia

*Corresponding Author, Received: 11 July 2023, Revised: 20 Sep. 2023, Accepted: 24 Sep. 2023

ABSTRACT: The assessment of liquefaction potential after an earthquake is important to understanding earthquake risks to coastal infrastructure, thereby making it a secondary impact of seismic events. Therefore, this research compared liquefaction potential in Labuan Bajo waterfront area using various parameters, with a focus on earthquake return period to gauge liquefaction conditions in different seismic scenarios. Three earthquake scenarios with return period of 50 years, 100 years, and 2500 years were analyzed and used to evaluate potential for liquefaction under varying seismic conditions. A semi-empirical procedure was used to evaluate liquefaction potential in ten boreholes situated along Labuan Bajo waterfront. This assessment considered factors such as the Cyclic Stress Ratio (CSR) and Cyclic Resistance Ratio (CRR). Peak Ground Acceleration (PGA) and moment magnitude values were derived from the seismic code provided by the Ministry of Public Works and Housing of Indonesia. Meanwhile, the moment magnitude used for frequent earthquake was determined based on historical earthquake data around Labuan Bajo using Zmap 7.1. The results showed that liquefaction occurred with an SPT (Standard Penetration Test) value of 8, 18 and 31 for 50, 100 and 2500-year return period. When comparing Liquefaction Potential Index (LPI) values for each location, it became evident that BH-03 and BH-04 exhibited high values of 38.69 and 39.86, respectively, in the 50-year return period scenario. By using three parameters, the locations with high liquefaction potential can be determined precisely and mitigation can be planned early.

Keywords: Liquefaction, Frequent Earthquake, Return Period, Liquefaction Potential Index, Waterfront

1. INTRODUCTION

Soil liquefaction is a phenomenon in which a cohesionless saturated or partially saturated soil significantly loses its strength and stiffness, in response to an applied stress [1]. This occurrence can have substantial impacts, specifically on wharves and structures located near waterfront. When liquefaction takes place, the underlying soil loses its strength and transforms into a liquid-like state, resulting in the sinking or tilting of the upper structures or foundations [2-4]. This can lead to extensive damage as well as weaken the stability and operational effectiveness of these structures.

The Indonesian government, through the Ministry of Public Works and Housing, has embarked on a significant developmental project along Labuan Bajo waterfront area. This development aims to establish Labuan Bajo as a gateway to Komodo National Park, thereby attracting a huge number of tourists. Labuan Bajo is situated in a seismically active region [5], which heightens the vulnerability of this area to earthquake hazards.

Potential for liquefaction as a secondary disaster also requires thorough analysis. According to [6], Labuan Bajo is situated within a zone categorized by moderate to high vulnerability to liquefaction. Liquefaction vulnerability zone map serves as an initial source of information, primarily intended for regional development planning purposes and offering a broader-scale assessment of possible occurrences. To accurately assess liquefaction risks in the specific waterfront area of Labuan Bajo, a more detailed analysis is essential. Unfortunately, such a comprehensive assessment has not been conducted yet, indicating the urgent need for further investigations to better understand and effectively address the specific liquefaction risks associated with this location.

When assessing liquefaction potential, often based on probabilistic estimates such as a 2% probability of occurrence in 50 years or 2500-year return period [7]. According to Green and Boomer [10], a magnitude of 4.5 is considered significant enough to potentially trigger liquefaction. Other research also reported that a Peak Ground Acceleration (PGA) value of 0.096 g can potentially serve as a threshold for initiating liquefaction [11].

In order to ensure the accuracy of design planning analysis and prevent overestimation, it is essential to compare the effects of maximum earthquake with those of more frequent occurrences. This analytical method is instrumental in evaluating potential susceptibility of the site to liquefaction across various seismic scenarios. It takes into account the regularity and intensity of seismic activity, thereby facilitating a more accurate assessment of liquefaction hazard. The subsequent sections of this research provide a comprehensive explanation of these seismic scenarios.

2. RESEARCH SIGNIFICANCE

Understanding liquefaction potential is important for the development of area located in earthquake-prone regions. This knowledge allows for the implementation of suitable soil reinforcement methods and structural designs to mitigate earthquake-induced damages. The present research provides an overview of liquefaction potential by considering various earthquake parameters as a preliminary step in assessing the susceptibility of existing buildings based on available data. The results tend to provide valuable insights for local governments, aiding in effectively implementing measures for mitigating liquefaction-related disasters.

3. GEOLOGICAL AND SEISMICITY OF RESEARCH AREA

Labuan Bajo is a town located on the western tip of Flores Island in Indonesia, and it also serves as the gateway to Komodo National Park. In terms of geological features, this area exhibits a diverse range of formations. The coastal plains and deposits are primarily composed of alluvial formations (Qa). The northern region is comprised of a rugged and hilly topography characterized by tuffaceous dacite (Tmdt) and layered limestone formations (Tml) [12].

The calculations were based on soil investigation data obtained in 2020, and these were conducted twice, yielding consistent results. Based on the soil investigation analysis carried out in the research area (Fig. 1), the following boreholes BH-01, BH-02, BH-03, BH-04, and BH-07 predominantly exhibited sand layers ranging from soft to medium consistency while the rest contained clay and rock. Additionally, the groundwater elevation rises above the ground surface during high tides.

Labuan Bajo located along the Pacific Ring of Fire, frequently experiences earthquake due to the influence of two geological features responsible for significant seismic events. The first of these features is the subduction zone located in the southern area, where Eurasia and Indo-Australian tectonic plates interact, with one plate subducting beneath the other. The second is the flores back-arc thrust fault located towards the north [13]. A visual representation of earthquake distribution in Labuan Bajo, sourced from earthquake.usgs.gov website, with a radius of 200 *km* from the location of the research site is shown in Figure 2.

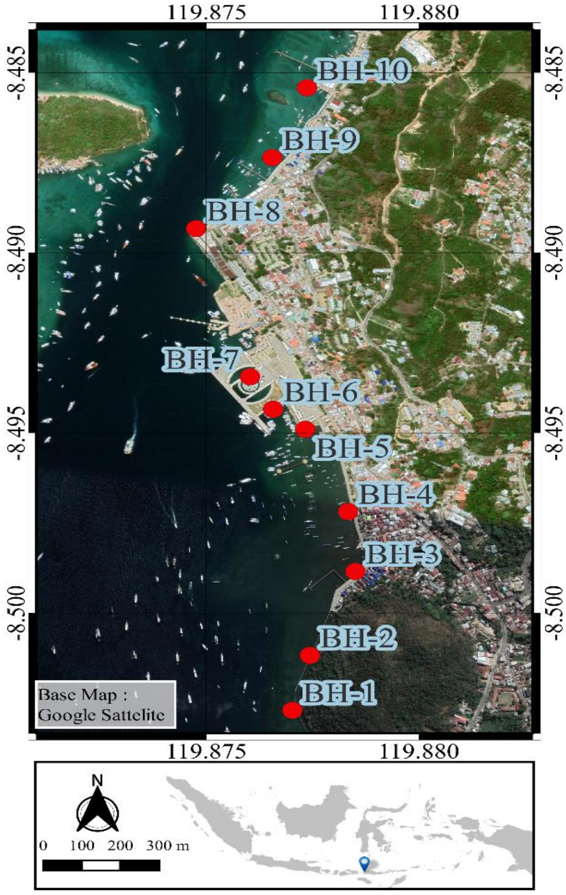

Fig. 1 Borehole location along the waterfront area

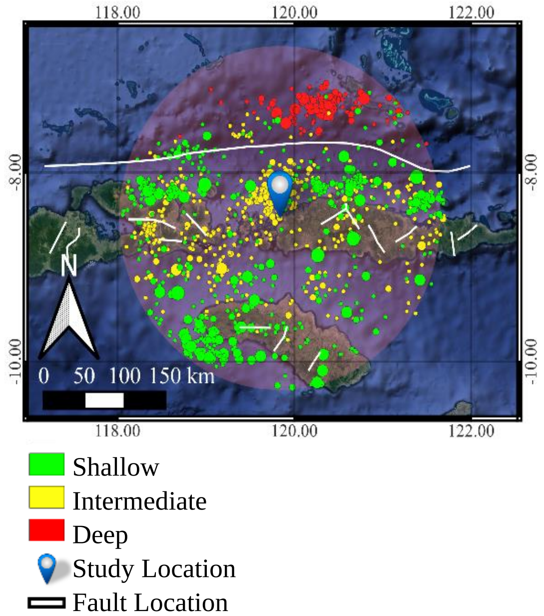

Fig. 2 Earthquake distribution in 200 km radius around Labuan Bajo

4. METHODS

The research quantitatively compared the impact of earthquake on liquefaction potential through a structured process comprising three key stages: data collection, safety factor value determination, and Liquefaction Potential Index (LPI) calculation. The effects of earthquake on liquefaction potential were compared quantitatively. The stages carried out are collecting data, determining the safety factor value and LPI value.

Earthquake selection was based on a classification system that categorizes seismic events according to their frequency and return period [14]. Furthermore, two primary return period were considered 50 and 100 years. The selection of a 50-year return period corresponds to earthquake categorized as frequent, indicating a higher likelihood of occurrence within a relatively short time frame. Similarly, the adoption of a 100-year return period is in line with earthquake classified as occasional, signifying events with a lower likelihood of occurrence but still significant in terms of their impact. The inclusion of a 2500-year return period represents the Maximum Considered Earthquake (MCEr) for building design purposes. This extended return period accounts for extreme seismic events expected in the region under consideration, ensuring that the analysis accounts for the worst-case scenario.

The process of determining seismic site class adheres to the guidelines stated in [7]. This classification relies on the calculation of SPT values, a computation performed using Eq. 1. Classification was carried out to estimate site coefficient amplification as shown in Table 1. The amplification factor, influenced by local soil conditions, is calculated using Eq. 2.

$$\bar{N} = \frac{\sum_{i=1}^{n} d_i}{\sum_{i=1}^{n} \frac{d_i}{N_i}} \tag{1}$$

$$PGA_M = F_{PGA} \, . PGA \tag{2}$$

where d_i = soil layer thickness, $\bar{N}$ = standard penetration resistance, PGA_M = PGA influenced by site class, and F_{PGA} = site coefficient.

Table 1 Site coefficient [7]

Site Class	PGA≤ 0.1*g*	PGA= 0.2*g*	PGA= 0.3*g*	PGA= 0.4*g*	PGA≥ 0.5*g*
SA	0.8	0.8	0.8	0.8	0.8
SB	1.0	1.0	1.0	1.0	1.0
SC	1.2	1.2	1.1	1.0	1.0
SD	1.6	1.4	1.2	1.1	1.0
SE	2.5	1.7	1.2	0.9	0.9
SF	Required specific site response analysis				

The PGA used in this research was determined based on specific return period. This return period were obtained from the seismic code mandated by the Indonesian government, which provides detailed guidelines for evaluating anticipated ground acceleration levels in different regions throughout the country.

Liquefaction potential analysis was conducted using a semi-empirical procedure proposed by [15]. To calculate liquefaction potential for each soil layer, the analysis focused on determining the safety factor (SF) value. Soil layers were deemed susceptible to liquefaction when their safety factor value was less than 1.

The Safety Factor was calculated by comparing the cyclic stress ratio (CSR) with the cyclic resistance ratio (CRR) of the soil layer as stated in Eq. 3.

$$SF = \frac{CRR_{M,\sigma v'}}{CSR} \tag{3}$$

The CSR is a value that represents the ratio between the average cyclic shear stress (τ_{cyc}) and the effective overburden pressure ($\sigma_{v'}$) obtained using Eq. 4.

$$CSR = \frac{\tau_{cyc}}{\sigma_v'} = 0.65 \, r_d \, \frac{\sigma_v}{\sigma_v'} \, \frac{\alpha_{max}}{g} \tag{4}$$

where σ_v is total vertical stress, σ_v is the effective vertical stress, α_{max} is the maximum ground surface acceleration, and r_d is the stress reduction factor.

In order to determine the average cyclic shear stress (τ_{cyc}), it is necessary to consider the stress reduction factor. Eq. 5 to 7 can be used to calculate the stress reduction factor.

$$r_d = exp[\alpha(z) + \beta(z)M] \tag{5}$$

$$\alpha = -1.012 + 1.126 \, sin\left(\frac{z}{11.73} + 5.133\right) \tag{6}$$

$$\beta = 0.106 + 0.188 \, sin\left(\frac{z}{11.28} + 5.142\right) \tag{7}$$

In Eq. 6 and 7, the variable z represents the depth beneath the ground surface, and M denotes earthquake moment magnitude. In addition, the angle unit used is in radians.

The CRR value represents the soil resistance to liquefaction. Idriss and Boulanger [15] provided a CRR value correlation for a magnitude of 7.5 and an effective overburden pressure of 1 *atm*. This correlation included an adjustment based on the SPT values for equivalent clean sand $(N_1)_{60cs}$. These values are calculated using Eq. 8.

$$CRR_{M=7.5,\sigma v'=1atm} = exp\left(\frac{(N_1)60cs}{14.1} + \left(\frac{(N_1)60cs}{126}\right)^2 - \left(\frac{(N_1)60cs}{23.6}\right)^3 + \left(\frac{(N_1)60cs}{25.4}\right)^4 - 2.8\right) \tag{8}$$

After obtaining the $CRR_{M=7.5,\ \sigma v'=1atm}$, it was necessary to calculate the CRR under varying conditions of M and $\sigma_{v'}$ to adapt to the field conditions using Eq. 9.

$$CRR_{M,\sigma v'} = CRR_{M=7.5,\sigma v'=1atm} . MSF . K_\sigma \tag{9}$$

K_σ represents the effective overburden stress while Magnitude Scaling Factor (MSF) is used to account for the influence of ground motion duration on liquefaction initiation. MSF value was determined using Eq. 10 and 11.

$$MSF = 1 + (MSF_{max} - 1) * \left(8.64\, exp\left(\frac{-M}{4}\right) - 1.325\right) \tag{10}$$

$$MSF_{max} = 1.09 + \left(\frac{(N_1)_{60cs}}{31.5}\right)^2 \leq 2.2 \tag{11}$$

Considering the possible occurrence of the water table rising above the ground surface during high tide conditions, liquefaction potential calculation takes into account a scenario where both are at the same level.

Liquefaction potential of each borehole was determined using LPI. This method predicts potential levels based on the thickness and depth of soil layers susceptible to liquefaction near the ground surface. The formula for calculating potential is stated in Eq. 12.

$$LPI = \int_1^{20} F(z).w(z).dz \tag{12}$$

where $F(z) = 1 - FS$ for $FS < 1$, and $F(z) = 0$ for $FS \geq 1$. Then $w(z) = 10 - 0.5z$ with z in meter. The level of potential liquefaction levels proposed by [16], is shown in Table 2.

Table 2 LPI (Sonmez, 2003)

Liquefaction Index	Liquefaction Potential
0	Non-Liquefied
$0 < LPI \leq 2$	Low
$2 < LPI \leq 5$	Moderate
$5 < LPI \leq 15$	High
$15 < LPI$	Very High

Index values obtained were compared across all scenarios to identify vulnerable points that require thorough attention for mitigation purposes.

5. RESULTS AND DISCUSSIONS

The results of the site classification calculation revealed the distribution of different classes within the research area as shown in Table 4 and Table 5. Specifically, BH-01, BH-08, and BH-09 were classified as Site Class SD ($15 \leq \bar{N} \leq 50$), indicating a relatively stable and dense soil condition. BH-10 was classified under Site Class SC ($50 \leq \bar{N}$), representing a moderately stable soil condition. The remaining locations were classified as Site Class SE ($\bar{N} \leq 15$). indicating a soft soil condition.

The PGA values at the bedrock were determined for each scenario, using [17] for the 50-year return period and [18] for the remaining ones. These calculations yielded PGA values of 0.1 *g*, 0.15 *g*, and 0.4 *g* for the 50-year, 100-year, and 2500-year return period, respectively. Based on the results of the calculations, it was observed that the PGA values for each scenario and borehole exhibit certain variations. These variations are dependent on the site class and the specific bedrock PGA. These variations arise due to the inherent differences in soil characteristics and their effects on ground motion amplification. PGA_M calculations for each scenario in different seismic site classes are shown in Table 3.

To obtain conditions that resemble those in the field, earthquake magnitude parameter for frequent occurrence (50-year return period) was calculated using Zmap 7.1. This calculation was based on historical earthquake data from 1823 to 2023 (200 years), sourced from earthquake.usgs.gov. The resulting earthquake magnitude serves as a representative value for frequent seismic events. Based on Figure 3, the magnitude obtained for frequent earthquake is 4.6 M_w.

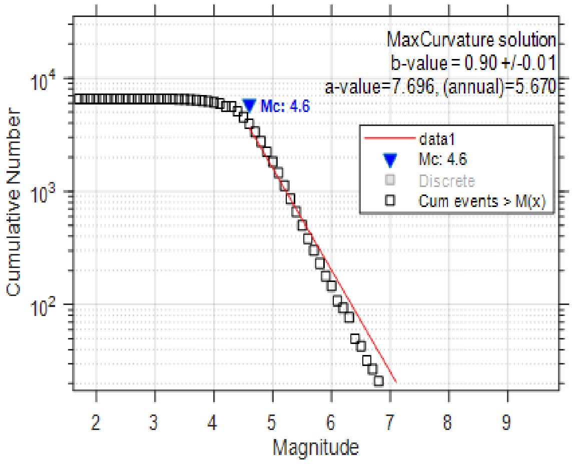

Fig. 1 Magnitude of completeness value obtained from Zmap analysis

For the 100-year and 2500-year return period, earthquake magnitudes were determined using available disaggregation maps [18]. Based on these maps, the magnitude values for each return period were obtained as 6.2 *Mw* and 6.4 *Mw*.

When calculating liquefaction potential for the 50-year return period, a range of safety factor values for the liquefiable layers was observed starting from 0.29, Additionally, the SPT values, were found between 2 to 8, with depths ranging from 0 to 14 *m*. The deepest layer to experience liquefaction was located within BH-03 at a depth of 14 *m* with a safety factor value of 0.66.

In the 100-year return period scenario, the lowest safety factor value for liquefiable soil is 0.20. The maximum SPT value for liquefiable soil is 18. The deepest liquefiable layer was found at a depth of 18 *m* within BH-03.

Table 3 SPT value and site class determination for BH-01, BH-02, BH-03, BH-04 and BH-05

Depth (*m*)	BH-01		BH-02		BH-03		BH-04		BH-05	
	SPT		SPT		SPT		SPT		SPT	
2	4	Fine Sand	4	Fine Sand	2	Fine Sand	3	Fine Sand	3	Fine Sand
4	22	Fine Sand	24	Fine Sand	3	Fine Sand	4	Fine Sand	5	Fine Sand
6	8	Medium Sand	6	Medium Sand	4	Fine Sand	5	Fine Sand	15	Clayey Silt
8	5	Medium Sand	5	Medium Sand	4	Fine Sand	4	Fine Sand	14	Clayey Silt
10	12	Medium Sand	12	Medium Sand	5	Fine Sand	6	Fine Sand	13	Clayey Silt
12	17	Medium Sand	17	Medium Sand	11	Medium Sand	12	Medium Sand	16	Clayey Silt
14	38	Medium Sand	37	Medium Sand	8	Medium Sand	11	Medium Sand	16	Clayey Silt
16	26	Medium Sand	28	Medium Sand	16	Medium Sand	17	Medium Sand	18	Silty Clay
18	31	Medium Sand	30	Medium Sand	18	Medium Sand	25	Medium Sand	26	Silty Clay
20	30	Medium Sand	29	Medium Sand	26	Medium Sand	29	Medium Sand	38	Coral
22	29	Medium Sand	29	Medium Sand	31	Medium Sand	33	Medium Sand	60	Sandy Silt
24	45	Medium Sand	46	Medium Sand					59	Sandy Silt
26	60	Medium Sand	60	Medium Sand						
$\bar{N}$	15.52		14.94		7.74		9.75		14.60	
Site Class	SD		SE		SE		SE		SE	

Table 4 SPT value and site class determination for BH-06, BH-07, BH-08, BH-09 and BH-10

Depth (*m*)	BH-06		BH-07		BH-08		BH-09		BH-10	
	SPT		SPT		SPT		SPT		SPT	
2	2	Clayey Sand	2	Sandy Clay	3	Fine Sand	3	Fine Sand	15	Fine Sand
4	3	Clayey Sand	4	Sandy Clay	5	Fine Sand	5	Fine Sand	22	Silty Clay
6	4	Clayey Sand	5	Fine Sand	14	Silty Clay	24	Silty Clay	32	Silty Clay
8	12	Clayey Sand	5	Fine Sand	21	Silty Clay	35	Silty Clay	60	Rock
10	34	Silty Clay	6	Fine Sand	29	Silty Clay	49	Silty Clay	60	Rock
12	28	Silty Clay	22	Fine Sand	32	Silty Clay	54	Silty Clay	60	Rock
14	34	Silty Clay	21	Fine Sand	34	Silty Clay	57	Silty Clay		
16	38	Silty Clay	18	Fine Sand	42	Silty Clay	60	Silty Clay		
18	42	Silty Clay	15	Fine Sand	54	Silty Clay				
20	60	Sandy Silt	23	Fine Sand	60	Silty Clay				
22	60	Sandy Silt	14	Fine Sand						
24	60	Sandy Silt	28	Fine Sand						
26	60	Sandy Silt	22	Fine Sand						
28			32	Fine Sand						
30			33	Fine Sand						
$\bar{N}$	10.89		8.38		18.60		22.17		77.57	
Site Class	SE		SE		SD		SD		SC	

Table 5 PGA_M calculation for each scenario in different seismic site class

Return Period		PGA (*g*)	F_{PGA}	PGA_M (*g*)
	SC		1.4	0.14
50-year	SD	0.1	1.6	0.16
	SE		2.4	0.24
	SC		1.25	0.18
100-year	SD	0.15	1.5	0.22
	SE		2.15	0.32
	SC		1.2	0.48
2500-year	SD	0.4	1.2	0.48
	SE		1.4	0.56

A significant observation was seen in the scenario corresponding to a 2500-year return period, almost all sand layers experienced liquefaction. Particularly, BH-03 exhibited the lowest safety factor and highest SPT values of 0.11 and 31, respectively among the identified liquefiable soil layers.

The results of the safety factor for the sand layer from BH-01 to BH-06, are shown in Figure 4, BH-07 to BH-09 shown in Figure 5. The results of the safety factor specifically for BH-10 with depth in *m* are shown in Figure 6. These figures provide visual representations of the calculated safety factors.

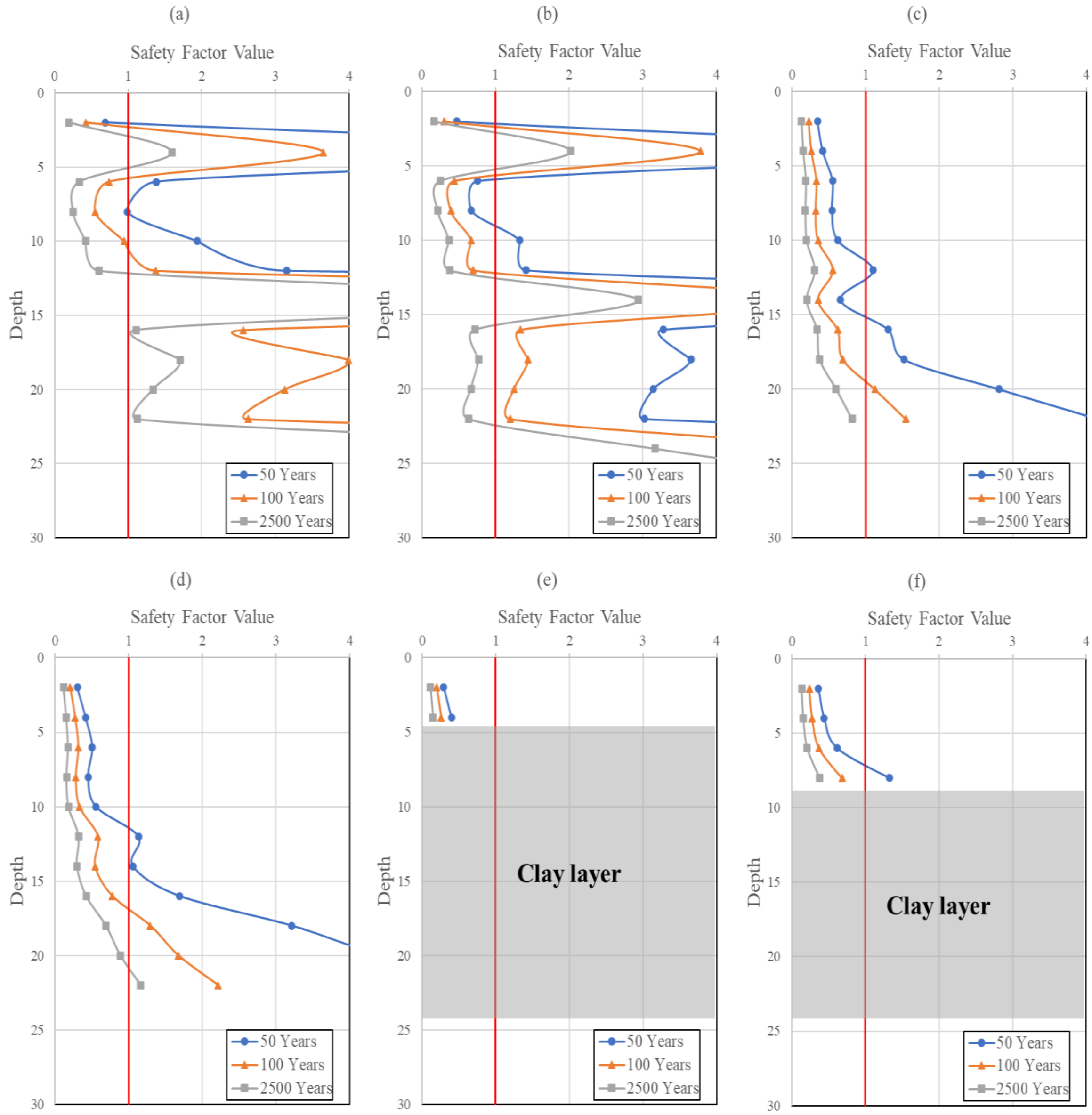

Fig. 2 Safety factor for each scenario and borehole (a) BH-01, (b) BH-02, (c) BH-03, (d) BH-04, (e) BH-05, (f) BH-06

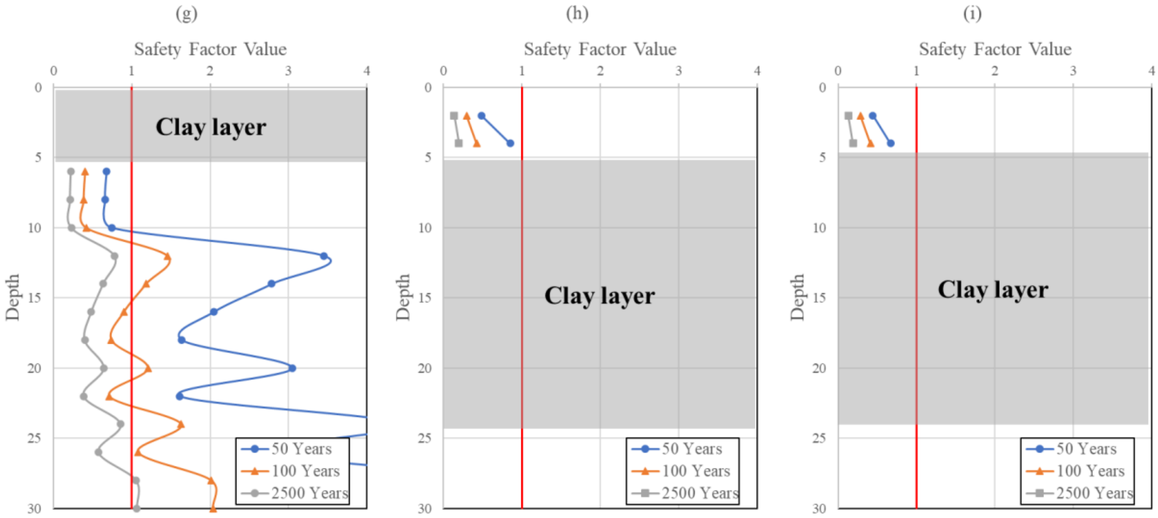

Fig. 3 Safety factor for each scenario and borehole (g) BH-07, (f) BH-08 and (i) BH-09

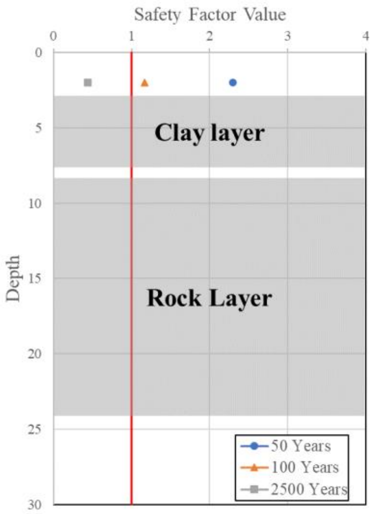

Fig. 6 Safety factor for borehole BH-10

Based on the evaluation of the LPI values for each borehole and scenario as shown in Table 6, distinct patterns were observed. It was noticed that six boreholes consistently exhibited an extremely high vulnerability to liquefaction across all scenarios. These specific locations, namely BH-02, BH-03, BH-04, BH-05, BH-06, and BH-09, consistently indicated a significant likelihood of experiencing liquefaction-induced ground failure. However, when examining the scenario with a 50-year return period earthquake, four other boreholes exhibited different levels of vulnerability. Among these, some boreholes were categorized as having a high liquefaction potential, while others were categorized as non-liquefied. Comparing the LPI values for each location, it was observed that BH-03 and BH-04 exhibited extremely high LPI values of 38.69 and 39.86, respectively, for the 50-year return period (frequent earthquake) scenario.

Table 5 LPI value and classification for a borehole in each return period scenario

Borehole	*LPI*					
	50-year return period		100-year return period		2500-year return period	
	LPI Value	Classification	LPI Value	Classification	LPI Value	Classification
BH-01	5.96	High	20.06	Very High	41.74	Very High
BH-02	16.89	Very High	33.47	Very High	47.71	Very High
BH-03	38.69	Very High	58.99	Very High	72.67	Very High
BH-04	39.86	Very High	57.99	Very High	71.84	Very High
BH-05	22.28	Very High	26.30	Very High	29.63	Very High
BH-06	25.86	Very High	37.84	Very High	47.59	Very High
BH-07	11.16	High	22.52	Very High	35.14	Very High
BH-08	11.76	High	21.96	Very High	28.44	Very High
BH-09	15.35	Very High	22.31	Very High	28.59	Very High
BH-10	0.00	No Liq	0.02	Low	10.07	High

The evaluation of liquefaction potential for frequent seismic events specifically those with a magnitude of 4.6 Mw, has yielded results. These results strongly suggest a high probability of liquefaction occurrence in such scenarios. They are consistent with the research conducted by Green and Boomer [10], who had previously reported that liquefaction susceptibility can be triggered by a 4.5 Mw earthquake.

In boreholes with consistent conditions for each scenario, the SPT values below 5 are found in layers at a depth lower than 8 *m*. This indicates that the soil layers at 8m are relatively weak or unstable. As a result, it leads to a low safety factor and high LPI value, indicating a greater potential geotechnical risk at that depth. Therefore, special attention is needed in the planning and execution of construction in that area to ensure the stability and safety of the structures being built.

6. LIMITATIONS

Limitations of the research include several factors. First and foremost, the study primarily relies on soil investigation data from 2020, potentially failing to capture evolving geological conditions. The use of a semi-empirical procedure introduces inherent uncertainties in predicting real-world liquefaction events. Moreover, the assumption of uniform soil properties within boreholes oversimplifies the complex reality of soil variability. Relying on historical earthquake data and seismic codes for magnitude and return period calculations may not encompass the full range of potential earthquake scenarios. The absence of real-time monitoring of soil conditions, groundwater levels, and seismic activity further limits the study's ability to provide a comprehensive assessment.

7. CONCLUSIONS

In conclusion, to evaluate liquefaction potential, three scenarios, each representing different earthquake return period, were considered. This method aimed to compare and assess the variations in liquefaction potential under distinct seismic conditions. By examining these scenarios, it was possible to analyze and understand potential for liquefaction occurrence at different levels of seismic activity.

LPI for each scenario resulted in different values. This indicated variations in potential for liquefaction across the research area. Despite the differing values, the overall assumption remained the same. The results from this research emphasized specific locations, labeled as BH-02, BH-03, BH-04, BH-05, BH-06, and BH-09, which consistently exhibited high liquefaction potential susceptibility across all three scenarios. This consistent result emphasized the need for further detailed investigation for to implement mitigation measures and engineering interventions. Such efforts were essential to enhance the resilience of structures and infrastructure within these vulnerable zones.

8. ACKNOWLEDGMENTS

The authors are grateful for the support and assistance provided by the Indonesian Ministry of Public Works and Housing throughout this research. Their valuable support has been instrumental in the successful execution of the research project.

9. REFERENCES

[1] Jefferies M., and Been K., Soil Liquefaction : Critical State Approach, Second Edition, CRC press, 2015, pp 1-690.

[2] Kardoğan P.S.Ö., and Bhattacharya S., Review of Liquefaction Around Marine and Pile-Supported Wharf Structures, In Proceedings of 3rd International Sustainable Buildings Symposium (ISBS 2017) Volume 1 3, Springer International Publishing, 2018, pp. 893-903.

[3] Cubrinovski M., Bray J.D., De La Torre C., Olsen M.J., Bradley B.A., Chiaro G., Stocks E. and Wotherspoon L., Liquefaction effects and associated damages observed at the Wellington CentrePort from the 2016 Kaikoura earthquake, Bulletin of the New Zealand Society for Earthquake Engineering, 50(2), 2017, pp.152-173.

[4] Lee C.J., Wen Y.H., Chen H.T., Yi C.T., Chin C.H., Yuan C.W., and Meng H.H., Seismic Responses Of Short Grouped-Piles Embedded In Liquefiable Sandy Soils During Earthquakes, GEOMATE Journal 8, no. 16 2015, pp 1218-1225.

[5] Irjan I, Luthfin A, and Hidayati S., Analysis of vulnerability to destructive tectonic earthquakes based on Zhao's attenuation function in East Nusa Tenggara, Indonesian Journal of Applied Physics 12, no. 2 2022, pp. 235-241 (In the Indonesian Language).

[6] Buana T. W., Hermawan R. N. W., Rahdiana R. W., Wahyudin G. Hasibuan, and Sollu W. P., Atlas of Liquefaction Vulnerability Zones in Indonesia, Geological Agency-Groundwater and Environmental Geology Center, 2019, pp. 31 (In the Indonesian Language).

[7] National Standardization Agency of Indonesia, National Standard for Designing

Earthquake Resistance for Buildings and Non-Buildings, SNI-03-1726-2019.
[8] Abdul Jalil, Teuku Faisal Fathani, Iman Satyarno, and Wahyu Wilopo., A Study On The Liquefaction Potential In Banda Aceh City After The 2004 Sumatera Earthquake. GEOMATE Journal 18 No.65, 2020, pp. 147-155.
[9] Amalia, K. P., Ismanti, S., & Saputra, A. Liquefaction Potential Evaluation In Toba Crater Indonesia. GEOMATE Journal, 25(110), 2023. pp. 123–131.
[10] Green Russell A., and Julian J. Bommer., What is the smallest earthquake magnitude that needs to be considered in assessing liquefaction hazard?, Earthquake Spectra 35, no. 3, 2019, pp. 1441-1464.
[11] de Magistris, F. S., Giovanni L., Giovanni F., and Giovanni F., A database for PGA threshold in liquefaction occurrence, Soil Dynamics and Earthquake Engineering 54 , 2013, pp. 17-19.
[12] Febriarta E., Susanto D., Wicaksono A., and Larasati A., Study of deterministic methods for landslide vulnerability zoning in Labuan Bajo East Nusa Tenggara, Majalah Geografi Indonesia 36, no. 1, 2022, pp. 41-50 (In the Indonesian Language).
[13] Rysnawati N., Sukarasa I. K, and Paramarta I., Analysis of earthquake hazard and vulnerability levels in the East Nusa Tenggara (NTT) region, Buletin Fisika 18, no. 1, 2017, pp. 32-37 (In the Indonesian Language).
[14] Seismology Committee-Structural Engineers Association of California, Recommended Lateral Force Requirements and Commentary, SEAOC Blue Book Seventh Edition 1999, California: Structural Engineers Association of California, 1999, pp. 320.
[15] Boulanger R.W. and Idriss I.M., CPT and SPT based liquefaction triggering procedures, Report No. UCD/CGM.-14 1, 2014, pp. 1-138.
[16] Sonmez H., Modification of the Liquefaction Potential Index and Liquefaction Susceptibility Mapping for a Liquefaction-Prone Area (Inegol, Turkey), Environmental Geology, Vol. 44, Issue 7, 2003, pp. 862–871.
[17] National Earthquake Research Center, Indonesia Earthquake Source and Hazard Map 2017, Pusat Litbang Perumahan dan Pemukiman-Ministry of Public Works and Housing, 2017, pp. 1-400 (In the Indonesian Language).
[18] National Earthquake Research Center, Deaggregation map of earthquake hazard in Indonesia for seismic-resistant infrastructure planning and evaluation, 2022, pp 222-240.